

## FTIR spectroscopy of Ti-rich pargasites from Lherz and the detection of O<sup>2-</sup> at the anionic O3 site in amphiboles

GIANCARLO DELLA VENTURA,<sup>1,2,\*</sup> ROBERTA OBERTI,<sup>2</sup> FRANK C. HAWTHORNE,<sup>3</sup>  
AND FABIO BELLATRECCIA<sup>1</sup>

<sup>1</sup>Dipartimento di Scienze Geologiche, Università Roma Tre, Largo S. Leonardo Murialdo 1, I-00146 Roma, Italy

<sup>2</sup>CNR-Istituto di Geoscienze e Georisorse, Unità di Pavia, via Ferrata 1, I-27100 Pavia, Italy

<sup>3</sup>Department of Geological Sciences, University of Manitoba, Winnipeg, R3T 2N2 Canada

### ABSTRACT

This paper reports a single-crystal unpolarized-light FTIR study in the OH-stretching region of a suite of well-characterized Ti-rich pargasites from Lherz (French Pyrenees). All amphiboles studied have fairly constant M-site composition, with <sup>61</sup>Al<sub>tot</sub> ~0.55 atoms per formula unit (apfu), <sup>61</sup>Ti ~0.45 apfu, and <sup>61</sup>Fe<sup>3+</sup> ~0.40 apfu. SIMS and SREF data show all samples to have an O3 anion composition of OH ≈ O<sup>2-</sup> ≈ 1.0 apfu, with negligible F. The FTIR spectra show for all samples a broad absorption consisting of several overlapping bands; three main components can be recognized: ~3710, 3686, and 3660 cm<sup>-1</sup>, respectively, with an asymmetric tail extending to lower frequency. Six Gaussian components can be fitted to the spectra; comparison with spectra of both synthetic and natural pargasites allows five of these components to be assigned to local configurations involving OH-O<sup>2-</sup> at the O3 site, thus showing that coupling with an O<sup>2-</sup> anion through an A-cation significantly affects band position. Infrared spectroscopy can detect the presence of O<sup>2-</sup> in amphiboles in chemically favorable cases, i.e., in the absence of F. Moreover, the FTIR spectra show that all octahedral configurations involving M<sup>1</sup>Ti<sup>4+</sup> or M<sup>1</sup>Fe<sup>3+</sup> M<sup>3</sup>Fe<sup>3+</sup> are associated with O<sup>2-</sup> at both adjacent O3 sites, and that M<sup>3</sup>Al is locally associated with OH, confirming SRO models based on structure refinement results.

**Keywords:** Ti-rich pargasite, Lherz (French Pyrenees), single-crystal FTIR spectroscopy, anion occupancy

### INTRODUCTION

Amphiboles are a complex group of hydroxyl-bearing minerals in which solid solution may occur at all cation sites, and also at the anion site O3, which may be occupied by OH<sup>-</sup>, F<sup>-</sup>, Cl<sup>-</sup>, and O<sup>2-</sup>. For O3 = O<sup>2-</sup>, local bond-valence requirements are satisfied by the occurrence of highly charged octahedral cations occurring either at the adjacent M1 site (Ti) or at the M1 and M3 sites (Fe<sup>3+</sup> and Mn<sup>3+</sup>). Amphiboles may crystallize with variable amounts of monovalent (OH<sup>-</sup>, F<sup>-</sup>, Cl<sup>-</sup>) and divalent (O<sup>2-</sup>) anions at O3, but loss of hydrogen may also occur post-crystallization due, for instance, to an increase in *T* or decrease in *P* (e.g., during subduction processes or volcanic eruptions). In the latter case, extensive experimental studies on dehydrogenation obtained by thermal treatment in both natural and synthetic amphiboles (e.g., Barnes 1930; Addison et al. 1962a, 1962b; Ernst and Wai 1970; Ungaretti 1980; Phillips et al. 1989; Popp et al. 1995a, 1995b) have shown that the amount of O<sup>2-</sup> is correlated with the amount of Fe<sup>3+</sup> produced by the accompanying oxidation. Much of this work was done using Mössbauer or infrared spectroscopy as probes to monitor the change in iron oxidation state, loss of H, and atomic adjustments within the structure, such as displace-

ment of Na from the M4 site to the A site in sodic amphiboles (e.g., Ernst and Wai 1970).

Systematic analysis of natural amphiboles shows that crystals with major amounts of O<sup>2-</sup> at O3 contain major amounts of Ti<sup>4+</sup> and Fe<sup>3+</sup>. The association between Ti<sup>4+</sup> and OH-deficiency has long been recognized in calcic amphiboles (kaersutites, with Ti > 0.50 atoms per formula unit, apfu; Leake 1968; Saxena and Ekstrom 1970), and neutron-diffraction refinement (Kitamura and Tokonami 1971; Kitamura et al. 1973, 1975; Jirak et al. 1986; Pechar et al. 1989) has shown that Ti is partly or completely ordered at the M1 site. More recently, Oberti et al. (1992) showed significant amounts of O<sup>2-</sup> at O3 in sodic-calcic amphiboles (richterites), where it occurs via the mechanism M<sup>1</sup>Ti<sup>4+</sup> + 2 O<sup>3</sup>O<sup>2-</sup> → M<sup>1</sup>(Mg,Fe<sup>2+</sup>) + 2 O<sup>3</sup>OH<sup>-</sup>. Hawthorne et al. (1998) showed a strong inverse correlation between Ti<sup>4+</sup> and the OH content at O3 determined by SIMS (secondary-ion mass spectrometry) on a suite of sodic to sodic-calcic amphiboles from Coyote Peak, California. However, stoichiometrically hydrogen-deficient amphiboles with new root compositions have been found only in the sodic amphibole group: ungarettiite, NaNa<sub>2</sub>Mn<sub>2</sub><sup>2+</sup>Mn<sub>3</sub><sup>3+</sup>Si<sub>8</sub>O<sub>22</sub>O<sub>2</sub>, Hawthorne et al. (1995); obertiite, NaNa<sub>2</sub>Mg<sub>3</sub>Fe<sup>3+</sup>TiSi<sub>8</sub>O<sub>22</sub>O<sub>2</sub>, Hawthorne et al. (2000a); dellaventuraite, NaNa<sub>2</sub>LiMgMn<sub>3</sub><sup>3+</sup>TiSi<sub>8</sub>O<sub>22</sub>O<sub>2</sub>, Tait et al. (2005). To sum up, the association of a highly charged octahedral cation with O<sup>2-</sup> at O3 is a widespread feature in amphiboles.

\* E-mail: dellaven@uniroma3.it

However, correct estimation of the OH content is still extremely difficult, and can be achieved only with well-calibrated ion-microprobe analysis (SIMS) or by careful single-crystal structure refinement (SREF) and structure modeling. In the former case, the amount of  $O^{2-}$  can be calculated on the basis of the H, F, and Cl contents as  $O^{2-} = 2 - (OH + F + Cl)$ .

Robert et al. (1999) have shown that the anion substitutions such as the  $^{3}OH_1$   $^{3}F_1$  exchange have a significant effect on the infrared spectrum of amphiboles; in particular, samples with occupied A sites show the appearance of a discrete band due to local OH-F arrangements, whose intensity is proportional to the OH/F ratio.

We present here a spectroscopic study of a well-characterized suite of Ti-rich  $O^{2-}$ -bearing pargasites from a metasomatized peridotite from Lherz (French Pyrenees; Zanetti et al. 1996). We show that the effect of  $O^{2-}$  on the infrared spectrum is similar to that of F, implying that, in favorable cases (i.e., in F-free samples), infrared spectroscopy is a valuable tool, in combination with SREF and/or EMP + SIMS, to characterize the degree of hydrogen deficiency in amphiboles and to derive structural patterns of local cation-anion associations.

### STUDIED SAMPLES

The amphibole crystals used in this work were characterized by Zanetti et al. (1996). The host rock is a metasomatized peridotite (spinel lherzolite) from Lherz (French Pyrenees), containing a thin (1.3 cm) hornblende vein with sharp boundaries against the host peridotite. The amphibole crystals were extracted from inside the vein, and from the host peridotite at increasing distances (up to 4 cm) from the vein. A combination of EMP (electron microprobe) + SIMS microanalysis (for major and trace elements) and SREF showed all amphiboles to be Ti-rich pargasite of fairly constant M-site composition, with  $^{6}Al_{tot} \sim 0.55$ ,  $^{6}Ti \sim 0.45$ , and  $^{6}Fe^{3+} \sim 0.40$  apfu. SIMS and SREF data also show all samples to have an O3 anion composition of  $OH \approx O^{2-} \approx 1.0$  apfu, with negligible F (max. = 0.06 apfu) and Cl (max. = 0.03 wt%). According to Zanetti et al. (1996), the H deficiency is locally balanced by the presence of both Ti at the M1 site and  $Fe^{3+}$  disordered over the M1 and the M3 sites, and the amount of (disordered) Al at the M3 site increases with the distance from the contact between the vein and the host peridotite (Table 1).

**TABLE 1.** Crystal-chemical formulae of the studied samples (from Zanetti et al. 1996)

Sample	V1	HR1	HR2	HR3	LH12
A: K	0.23	0.14	0.10	0.07	0.03
Na	0.77	0.86	0.90	0.93	0.96
M4: Na	0.15	0.11	0.11	0.11	0.12
Ca	1.74	1.76	1.78	1.80	1.76
Fe,Mg	0.11	0.13	0.11	0.09	0.12
M1: Mg	1.47	1.46	1.48	1.41	1.49
Ti	0.26	0.34	0.30	0.32	0.35
$Fe^{2+}$	0.27	0.07	0.22	0.01	0.04
$Fe^{3+}$	1.29	0.13	1.32	0.26	0.12
M2: Mg	0.45	1.30	0.41	1.37	1.38
Al	0.23	0.46	0.13	0.37	0.38
Ti	0.02	0.10	0.09	0.16	0.08
Cr	0.01	0.10	0.04	0.08	0.09
$Fe^{3+}$	0.75	0.03	0.01	0.01	0.06
Ni	0.09	0.01	0.70	0.01	0.01
M3: Mg	0.16	0.72	0.14	0.67	0.65
Al	2.13	0.12	0.16	0.15	0.19
$Fe^{2+}$	1.87	0.03	2.17	0.01	0.05
$Fe^{3+}$	4.00	0.13	1.83	0.17	0.11
T1: Si	0.99	2.20	4.00	2.18	2.25
Al	0.06	1.80	0.98	1.82	1.75
T2: Si	0.95	4.00	0.04	4.00	4.00
O3: OH		1.00	0.98	0.89	1.03
F		0.06		0.04	0.04
$O^{2-}$		0.94		1.07	0.93

### Fourier-transform infrared (FTIR) spectra

Unpolarized single-crystal spectra were collected at room  $T$  in the principal OH-stretching region on the same crystals used for SREF and microchemical analysis by Zanetti et al. (1996). The crystals were extracted from the original microprobe mount and doubly polished to thicknesses ranging from  $\sim 20$  to  $\sim 80$   $\mu m$ , depending on the size of the original mount. A NicPlan FTIR microscope equipped with a nitrogen-cooled MCT-A detector and a KBr beamsplitter was used; nominal resolution was  $4$   $cm^{-1}$  and 128 scans were averaged. The resulting spectra are shown in Figure 1. At first inspection, they are virtually identical, and show a broad absorption consisting of several overlapping bands; three main components can be recognized:  $\sim 3710$ ,  $3686$ , and  $3660$   $cm^{-1}$ , respectively, with an asymmetric tail extending to lower frequency.

The spectra collected for the Ti-rich pargasites from Lherz are significantly different from those of synthetic (e.g., Della Ventura et al. 1999; Fig. 2a) and natural (Della Ventura, unpublished data; Fig. 2b) pargasites, which typically show a double-band pattern. However, the spectra of Figure 1 are very similar to those of synthetic OH-F exchanged pargasites (Robert et al. 2000), the spectrum of the  $OH_{0.8}F_{1.2}$  term being shown in Figure 2d for comparison.

One point worth emphasizing here is that in Figure 2, we are comparing spectra from the literature collected on powders with spectra obtained during this work on randomly oriented single crystals, and the question is whether this comparison is meaningful. Tait et al. (2001) studied, using a combination of structure refinement and FTIR spectroscopy, a gem-quality F-rich pargasite from the Baffin Island; they showed that the powder and unpolarized-light single-crystal infrared spectra collected on the same sample are identical in terms of relative intensity of the absorption bands, the single-crystal spectrum being only slightly better resolved into its component bands than the powder spectrum. Furthermore, polarized-light single-crystal FTIR data published in the literature (e.g., Skogby and Rossman 1991) and collected by us (unpublished) on several types of amphiboles show that changes in the crystallographic orientation of the sample with respect to the beam strongly affect the intensity of the whole pattern, while the relative intensity of the individual components in the spectrum is virtually unaffected. From the above discussion, it is apparent that relative band intensities between powder and single-crystal spectra of amphiboles may be compared.

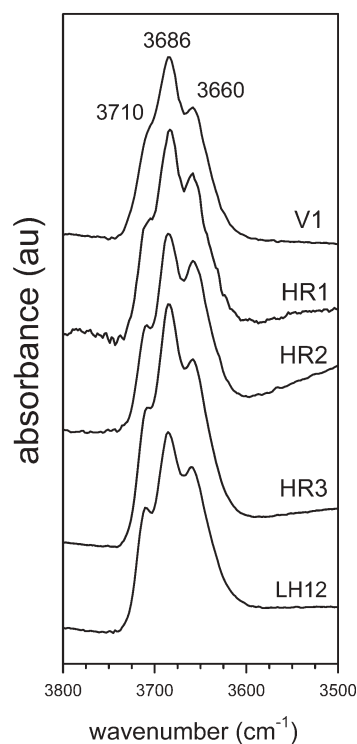


**FIGURE 1.** Single-crystal FTIR spectra of Ti-rich pargasites from Lherz.

### Fitting of the spectra

The digitized spectra of Figure 1 were fitted by interactive optimization followed by least-squares refinement, using the PeakFit program by Jandel (Della Ventura et al. 1996); the background was treated as linear, and all bands were modeled as symmetric Gaussians (Strens 1974). The spectrum was fitted by the smallest number of peaks needed for an accurate description of the profile, starting from the band parameters of Robert et al. (2000). Only individual full-width at half maximum height (FWHM) were constrained to be constant during refinement, and at convergence the results were very similar to those obtained by Robert et al. (2000) on synthetic (OH,F)-pargasite. A typical example of a fitted spectrum is given in Figure 3; it shows five main components, labeled A to E, plus one additional minor band at lower frequency (F), which was necessary to model the asymmetric tail of the absorption. Refinement results of the FTIR spectrum are summarized in Table 2 for sample HR3.

### LOCAL CONFIGURATIONS AROUND THE O3 SITE IN THE STUDIED SAMPLES

The crystal-chemical formulae of the studied samples, as determined by Zanetti et al. (1996), are reported in Table 1. The salient features to consider here are (1) all analyzed amphiboles have a full A site, with dominant Na and minor K; (2) Mg is virtually the only divalent octahedral cation ( $\text{Fe}^{2+} < 0.07$  apfu); (3)  $\text{Fe}^{3+}$  and Al are disordered within the strip of octahedra; in particular,  $\text{Fe}^{3+}$  is disordered over the M1 and M3 sites, whereas Al is disordered over the M2 and M3 sites. Previous work showed that the occurrence of  $\text{Fe}^{3+}$  at the M1 and M3 sites is related to the dehydrogenation process, whereas Al disorder occurs in pargasites with high Mg no. crystallized under high- $T$  conditions that do not show evidence of dehydrogenation [see Oberti et al. 1995, for more details and discussion on Pauling bond-strength (PBS) analysis]. (4)  $\text{Ti}^{4+}$  occurs at the M1 and M2 sites, with a strong preference for M1; (5) the anion composition  $\text{OH} \approx \text{O}^{2-} \approx$

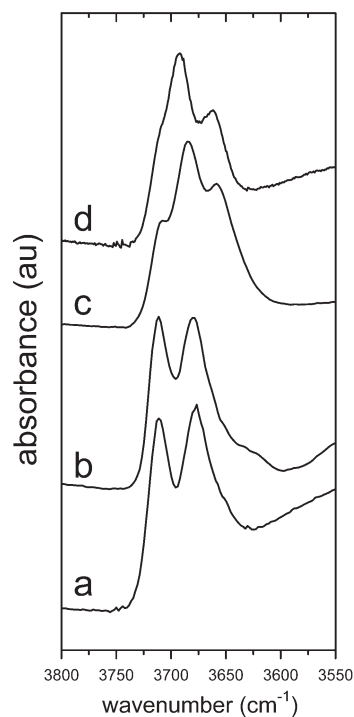


FIGURE 2. Comparison of (a) synthetic pargasite (Della Ventura et al. 1999), (b) pargasite from Finero (Della Ventura, unpublished data), (c) Ti-rich pargasite from Lherz (this work, sample HR3), and (d) synthetic  $(\text{OH}_{0.8}\text{F}_{1.2})$ -pargasite (Robert et al. 2000).

1.0 apfu allows all the possible OH-OH, OH- $\text{O}^{2-}$ , and  $\text{O}^{2-}$ - $\text{O}^{2-}$  local arrangements. Obviously, the local arrangement  $\text{O}^{2-}$ - $\text{O}^{2-}$  is invisible to infrared in the OH-stretching region, whereas OH-OH and OH- $\text{O}^{2-}$  are expected to give distinct spectroscopic signals in the OH-stretching region.

Figure 4 shows a schematic picture of the two M1 and the M3 octahedra sharing an O3 site. The case of a trimer of M sites associated with OH at O3 is shown on the right, and that of a trimer of M sites associated with  $\text{O}^{2-}$  at O3 is shown on the left. The A cation interacts with two O3 sites occurring in two distinct strips of octahedra and piling up along the  $a^*$  direction. Consider first the right side of Figure 4. Excluding  $^{\text{M1}}\text{Ti}$ , which must be locally associated with two adjacent  $\text{O}^{2-}$  within the same strip of octahedra (Oberti et al. 1992), the possibilities to be taken into consideration here are (1) the occurrence of Mg at M1 and/or M3; (2) of Al at M3; and (3) of  $\text{Fe}^{3+}$  at M1 and/or M3; the resulting arrangements are listed in Table 3. Arrangements 1 and 2 are both allowed; arrangement 3 could be either  $^{\text{M1}}\text{Mg}^{\text{M1}}\text{Fe}^{3+}\text{M}^3\text{Fe}^{3+}$  or  $^{\text{M1}}\text{Mg}^{\text{M1}}\text{Fe}^{3+}\text{M}^3\text{Al}$ , although neither is likely to occur due to their strong excess of bond-valence (expressed as PBS) at the O3 site. In addition, the arrangement  $^{\text{M1}}\text{Mg}^{\text{M1}}\text{Fe}^{3+}\text{M}^3\text{Fe}^{3+}$  will also involve  $\text{O}^{2-}$  at adjacent O3 sites, and is thus invisible to IR spectroscopy. Arrangement 4, with trivalent cations at all M1 and M3 sites, is also highly unlikely to occur.

Let us consider the situation where Ti (which is strongly ordered at M1 in natural environments, Tiepolo et al. 1999) is included in the list of cations at M1 and M3 (Fig. 4, left). Table 4 shows that most combinations involving Ti, except arrangement 1, have significantly high PBS, thus are unlikely to occur.

TABLE 2. Refined position, FWHM, and relative intensity (area%) for the IR bands of sample HR3

Band	Position ( $\text{cm}^{-1}$ )	FWHM ( $\text{cm}^{-1}$ )	Area%
A	3710	21	19
B	3687	22	30
C	3674	27	14
D	3657	26	24
E	3638	30	12
F	3612	28	1

TABLE 3. NN configurations adjacent to  $\text{O}^3\text{OH}^-$  in Ti-rich pargasite from Lherz (cf. Fig. 4)

	M1	M1	M3	$\Sigma$
1*	Mg	Mg	Mg	1.00
2*	Mg	Mg	$\text{M}^{3+}$	1.16
3	Mg	$\text{M}^{3+}$	$\text{M}^{3+}$	1.33
4	$\text{M}^{3+}$	$\text{M}^{3+}$	$\text{M}^{3+}$	1.50

Note:  $\text{M}^{3+} = (\text{Fe}^{3+}, \text{Al})$ ;  $\Sigma$  = calculated Pauling bond-strength incident at O3.

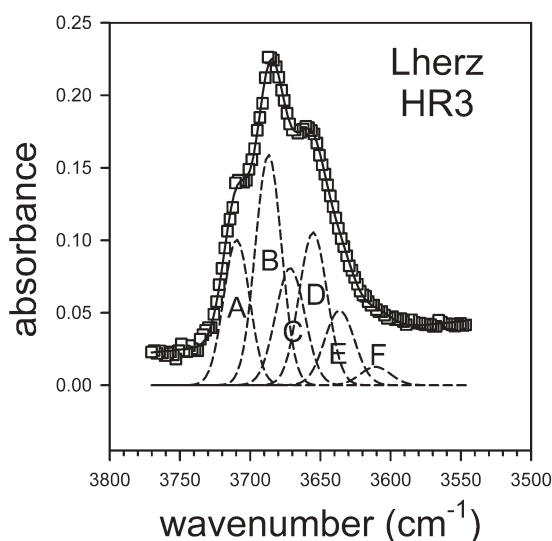
\* Arrangements most likely to occur (see text for detail).

TABLE 4. NN configurations adjacent to  $\text{O}^3\text{O}^{2-}$  in Ti-rich pargasite from Lherz (cf. Fig. 4)

	M1	M1	M3	$\Sigma$
1*	Ti	Mg	Mg	1.33
2	Ti	Mg	$\text{M}^{3+}$	1.50
3	Ti	$\text{M}^{3+}$	Mg	1.50
4	Ti	$\text{M}^{3+}$	$\text{M}^{3+}$	1.67
5	Ti	Ti	Mg	1.67
6	Ti	Ti	$\text{M}^{3+}$	1.84
7*	$\text{M}^{3+}$	Mg	Mg	1.16
8*	Mg	Mg	$\text{M}^{3+}$	1.16
9*	$\text{M}^{3+}$	Mg	$\text{M}^{3+}$	1.33
10	$\text{M}^{3+}$	$\text{M}^{3+}$	$\text{M}^{3+}$	1.50

Note:  $\Sigma$  = calculated Pauling bond-strength incident at O3.

\* Arrangements most likely to occur (see text for detail).



**FIGURE 3.** Example of spectrum fitting, sample HR3. The band labels (see text and Table 1) are also indicated. Open square = observed intensity; the line following the observed intensities is the envelope of the sum of the fitted component bands.

Actually, arrangement 2 might occur under high-*T* disordered conditions, but is unlikely due to the strong PBS excess. Other possibilities involve  $\text{Fe}^{3+}$  at M1 or M3 coupled with two divalent cations (arrangements 7 and 8 in Table 4), and  $\text{Fe}^{3+}$  at both M1 and M3 involving  $\text{O}^{2-}$  at both adjacent O3 sites (arrangement 9 in Table 4). These latter possibilities are expected to occur where the Ti content is less than half the amount of  $\text{O}^{3-}$ ; in this regard, it must be noted that, in the authors' experience,  $\text{Fe}^{3+}$  is preferentially incorporated at the M1 site.

Table 5 lists the possible local arrangements for sample HR3, calculated on the basis of the site-occupancies reported in Table 1. It is evident that combination of the available cations, according to the crystal-chemical constraints discussed above, results in only a small number of local arrangements. Specifically, arrangements 1 and 2 derive from the available  $\text{M}^1\text{Ti}$  and  $\text{M}^3\text{Fe}^{3+}$ ; the remaining  $\text{M}^1\text{Fe}^{3+}$  is then combined with Mg at M1 and M3 to give arrangement 3;  $\text{M}^3\text{Al}$  is associated with sufficient Mg to give arrangement 4; finally, all remaining Mg is combined to give arrangement 5. A point worth noting here is that only three of these arrangements involve OH-groups: arrangements 1 and 2 are each associated with 2  $\text{O}^{3-}$  each (Fig. 5a), and arrangement 3 is associated with one OH plus one  $\text{O}^{3-}$  (Fig. 5b), whereas arrangements 4 and 5 involve two OH groups, one on each side of the octahedral strip of octahedra (Fig. 5c). The information in Table 5 is in accord with the small number of bands in the OH-spectrum (Fig. 3).

#### BAND ASSIGNMENT

An important issue in the following discussion is the fact that monoclinic *C2/m* amphiboles with an occupied A site show two-mode behavior (in the OH-stretching region) with respect to anion solid-solutions, due to O-H vibrational coupling across the A-site cavity through the resident A atom (e.g., Robert et al. 1999). Thus, absorption by local arrangements involving an

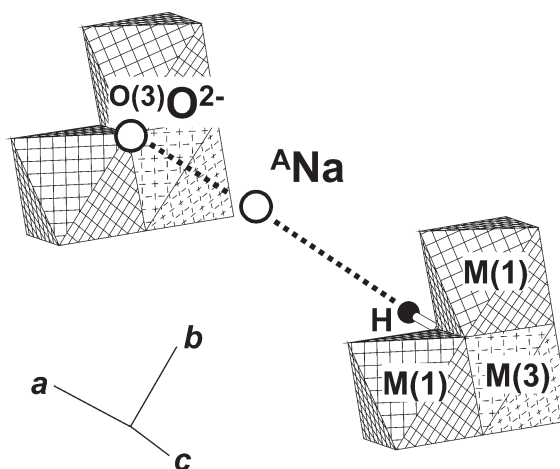


**FIGURE 4.** The local structure of the amphibole across the A site.

**TABLE 5.** Possible configurations at M(1,3) in sample HR3, and the coupled  $\text{O}^{3-}$  contents (see text for detail)

	M1	M1	M3	$\text{O}^{2-}$
1	0.32 Ti	0.32 Mg	0.32 Mg	0.64
2	0.17 $\text{Fe}^{3+}$	0.17 Mg	0.17 $\text{Fe}^{3+}$	0.34
3	0.09 $\text{Fe}^{3+}$	0.09 Mg	0.09 Mg	0.09
4	0.15 Mg	0.15 Mg	0.15 Al	–
5	0.27 Mg	0.27 Mg	0.27 Mg	–

OH group are significantly affected by adjacent arrangements involving a different O3 anion where locally associated with an occupied A site. This feature has been studied for  $\text{O}^3\text{F}^-$  (Robert et al. 1999, 2000; Della Ventura et al. 1993, 2001), but there are indications that the same is true for  $\text{O}^3\text{Cl}^-$ , and this work now shows that this mechanism also holds for  $\text{O}^3\text{O}^{2-}$ .

It is well established (see Hawthorne et al. 2005 for a complete list of references) that NN (nearest-neighbor) and NNN (next-nearest-neighbor) configurations around the O3 site affect both the frequency and the width of IR bands in the principal OH-stretching region. The possible types of NN and NNN configurations can be expressed using the notation M1M1M3-O3-A-T1T1 (Della Ventura et al. 1999; Hawthorne et al. 2005). This notation includes all the cation and anion arrangements, which are pertinent to the following discussion, namely the NN octahedrally coordinated M sites, the NNN tetrahedrally coordinated T sites, the NNN A site, and the O3 site itself. The composition of the T sites in the samples of this work (close to  $\text{Si}_6\text{Al}_2$ ), with Al strongly ordered at the T1 site (Table 1), implies that most (>90%) of the T1T1 dimers are SiAl, and thus we provisionally ignore this part of the notation in the following discussion. If we wish to consider the complete configuration, including adjacent anion groups coupled across the A site, the notation becomes: M1M1M3-O3-A-O3-M1M1M3. This notation does not include possible cation permutations at the M4 and M2 sites, which are also known to affect the OH-spectra (e.g., Della Ventura et al. 1999; Gottschalk et al. 1999; Hawthorne et al. 2000b, 2005). However, ~90% of the M4 sites are occupied by Ca in the studied samples. Moreover, the following discussion is focused on the anion substitutions, and a simplified model (which does not take

into account possible NNN effects due to the M2 and M4 site populations) is adequate for this purpose.

Assignment of the bands observed in the spectra (Fig. 3) is based on the large amount of infrared data now available for amphiboles. Band A can be unambiguously assigned to the local configuration MgMgMg-OH-Na-OH-MgMgMg (Semet 1973; Raudsepp et al. 1987; Della Ventura et al. 1999). Substitution of F for OH at the O3 site in both richterites and pargasites is correlated with the appearance of a new band in the OH-stretching spectrum, shifted toward lower frequency by  $\sim 15$   $\text{cm}^{-1}$  in richterite and  $\sim 20$   $\text{cm}^{-1}$  in pargasite (Robert et al. 1999, 2000; Della Ventura et al. 2001). This shift is due to changes in the interaction of the H atom with the Na atom: the presence of F allows further off-centering of Na, and reduces the cation-cation repulsion with the H proton bonded to the other strip of octahedra. We can assign band B, which is shifted by  $-23$   $\text{cm}^{-1}$  with respect to band A, to the local configuration MgMgMg-OH-Na-O<sup>2-</sup>-M1M1M3, where the three M octahedra on the right side of the configuration symbol must include either one Ti or two Fe<sup>3+</sup> to satisfy the local bond-valence requirements of O<sup>2-</sup> at O3.

Band C is shifted by approximately  $-35$   $\text{cm}^{-1}$  from band A; on the basis of the work of Della Ventura et al. (1999), it can be assigned to the local configuration MgMgAl-OH-Na-OH-MgMgAl.

Band D is shifted by  $-23$   $\text{cm}^{-1}$  with respect to band C, thus it can be assigned to the local configuration MgMgM<sup>3+</sup>-OH-Na-O<sup>2-</sup>-M1M1M3 (Della Ventura et al. 1999; Robert et al. 2000), where again the three M sites on the right side of the configuration symbol must include either one Ti or two Fe<sup>3+</sup>.

Assignment of band E (and F) is less straightforward. Due to its low frequency, the assignment should involve either configurations with Fe<sup>3+</sup> adjacent to OH, or the presence of some A-site empty environments (which should amount to  $\sim 5\%$  from the band intensity, see Hawthorne et al. 1997). Inspection of Table 5 suggests assignment of band E to the configuration Fe<sup>3+</sup>MgMg, which is associated with OH on one side of the strip, and O<sup>2-</sup> on the other side of the strip. However, in synthetic

magnesiohastingsite the Fe<sup>3+</sup>MgMg-OH band is shifted by  $-50$   $\text{cm}^{-1}$  relative to the corresponding MgMgMg-OH band (Semet 1973); band E is shifted by  $-72$   $\text{cm}^{-1}$  relative to the A band, suggesting that the OH-group bonded to the Fe<sup>3+</sup>MgMg trimer must be locally adjacent to O<sup>2-</sup>. The final band assignment is summarized in Table 6.

Comparison of Tables 5 and 6 shows that the relative intensities of bands A and C are in reasonable agreement with the calculated amounts of configurations 4 and 5 in the sample, and this provides a semi-quantitative check for the reliability of both the band assignments and the spectrum fitting procedure. Also, comparison of the intensity of the bands involving MgMgAl with the <sup>27</sup>Al content estimated based on structure refinement confirms that <sup>27</sup>Al is locally associated with two OH groups at the O3 sites.

A point to be noted is that the intensity of the B + D + E components, assigned to configurations involving OH-O<sup>2-</sup> arrangements, is  $\sim 66\%$  of the total intensity (Table 2). Considering that the anion composition of the sample is close to OH:O<sup>2-</sup> = 1:1 (Table 2), this suggests a random distribution of OH and O<sup>2-</sup> in the structure.

#### LOCAL ORDER IN TI-RICH PARGASITE FROM LHERZ

As discussed above, the OH-stretching spectra of the samples studied show local configurations involving both OH<sup>A</sup>Na<sup>A</sup>OH and OH<sup>A</sup>Na<sup>A</sup>O<sup>2-</sup> associations; the first direct implication is that, at least in chemically favorable cases (such as in the absence of F and significant amounts of Fe<sup>2+</sup>), FTIR spectroscopy is a valuable tool to detect O<sup>2-</sup> in amphiboles. The question now is whether we can use the OH-spectra to derive SRO information between cations and anions in amphibole.

Hawthorne (1997) and Hawthorne et al. (2005) have shown that local bond-valence requirements exert stringent controls on short-range configurations in the amphibole structure. Based on our present knowledge of amphibole crystal-chemistry, the following conclusions can be drawn for these pargasites from Lherz: (1) the octahedral configuration involving Ti<sup>4+</sup> associated with two O<sup>3</sup>O<sup>2-</sup> is M1M1M3 = Ti<sup>4+</sup>MgMg, as already proposed for obertiite (Hawthorne et al. 2000a) and dellaventurite (Tait

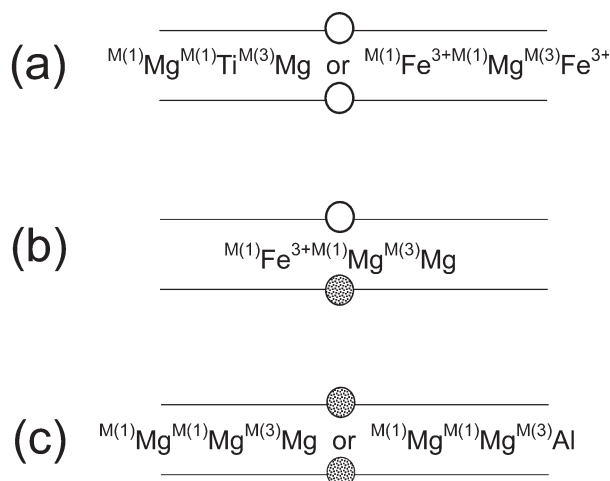


FIGURE 5. Sketch of the possible local arrangements between strips of octahedra piling along the  $a^*$ -direction and coupling through the A-site cation; hollow circle = O<sup>2-</sup>, pointed circle = OH<sup>-</sup>.

TABLE 6. Local configurations around the A site in Ti-rich pargasite from Lherz and the associated band in the IR spectrum

	Arrangement					Band
	M1M1M3	O3	A	O3	M1M1M3	
1	MgMgMg	OH	Na	OH	MgMgMg	A
2	MgMgAl	OH	Na	OH	MgMgAl	C
3	MgMgMg	OH	Na	OH	MgMgAl	A, C
4	MgMgMg	OH	Na	O <sup>2-</sup>	TiMgMg	B
5	MgMgMg	OH	Na	O <sup>2-</sup>	M <sup>3+</sup> MgM <sup>3+</sup>	B
6	MgMgAl	OH	Na	O <sup>2-</sup>	TiMgMg	D
7	MgMgAl	OH	Na	O <sup>2-</sup>	M <sup>3+</sup> MgM <sup>3+</sup>	D
8	Fe <sup>3+</sup> MgMg	OH	Na	O <sup>2-</sup>	TiMgMg	E
9	Fe <sup>3+</sup> MgMg	OH	Na	O <sup>2-</sup>	M <sup>3+</sup> MgM <sup>3+</sup>	E
10	TiMgMg	O <sup>2-</sup>	Na	O <sup>2-</sup>	TiMgMg	-
11	M <sup>3+</sup> MgM <sup>3+</sup>	O <sup>2-</sup>	Na	O <sup>2-</sup>	M <sup>3+</sup> MgM <sup>3+</sup>	-
12	M <sup>3+</sup> MgM <sup>3+</sup>	O <sup>2-</sup>	Na	O <sup>2-</sup>	TiMgMg	-

Note: Local arrangements 10, 11, and 12 do not involve OH, and hence do not produce any signature in this region of the infrared.

et al. 2005); (2) the octahedral configuration involving  $M^{3+}$  and associated with two adjacent  $O^3O^{2-}$  in the same strip of octahedra is  $M1M1M3 = M^{3+}MgM^{3+}$ ; this is the case in ungarrettiite (Hawthorne et al. 1995) and in experimentally dehydrogenated amphiboles; (3) the preferred octahedral configuration involving  $M^{3+}$  and associated with only one adjacent  $O^3O^{2-}$  in the same strip of octahedra is  $M1M1M3 = Fe^{3+}MgMg$ .

So far, we have considered the configurations  $M1M1M3-O3$  as if they were isolated entities. However, compositional implications arise when we consider how such configurations link together in the  $c$ -direction or how adjacent strips couple across the A site along the  $a^*$ -direction.

Consider for example the sequence of arrangements such as  $Ti^{4+}MgMg-O^{2-}$  and  $Fe^{3+}MgFe^{3+}-O^{2-}$ . As shown in Figures 6a and 6b these configurations can link in the  $c$ -direction without any change in composition, i.e., the aggregate compositions of the M1 and M3 cations and the O3 anion in the formula unit are  $Ti^{4+}MgMgO_3^{2-}$  and  $Fe^{3+}MgFe^{3+}O_3^{2-}$ , respectively. Consider next, the arrangement  $Ti^{4+}MgMg-O^{2-}$  in combination with the arrangement  $MgMgMg-OH$ . As indicated in Figure 6c, where the two arrangements are in a 1:1 relation, whatever type of local connectivity in the sequence, the  $O^{2-}$  content at O3 is always  $2 \times Ti^{4+}$ .

Consider now the arrangement  $Fe^{3+}MgFe^{3+}-O^{2-}$  (amount =  $x$ ) in combination with the arrangement  $MgMgMg-OH$  (amount =  $1 - x$ ). If the ratio between the arrangements is 1:1, the two arrangements may either alternate in a 1:1 sequence, as shown in Figure 6d, or connect in sequences involving all  $[Fe^{3+}MgFe^{3+}]-[Fe^{3+}MgFe^{3+}]$  and  $[MgMgMg-MgMgMg]$  linkages, with only one  $[Fe^{3+}MgFe^{3+}]-[MgMgMg]$  linkage, or any intermediate case between the two extreme situations. The resulting aggregate composition of the trimer is  $Fe^{3+}Mg_2O_3^{2-}OH_{-1}$ , i.e., the  $O^{2-}$  content at O3 is equal to the amount of the  $Fe^{3+}MgFe^{3+}$  arrangement. However, the local distribution of the O3 sites

occupied by  $O^{2-}$  will depend on the mutual connectivity of the arrangements. If the ratio is different, the aggregate composition will be a more complex function of  $x$  and  $(1 - x)$ , but the number of  $O^{2-}$  will always be equal to  $x$ . Combination of the  $[Ti^{4+}MgMg]$  and  $[Fe^{3+}MgFe^{3+}]$  arrangements obey the same rule, but all the O3 sites will be occupied by  $O^{2-}$ . To sum up, the local connectivity of the different arrangements may result in different aggregate compositions; however, for the studied samples, inspection of Table 2 shows that the compositions agree closely with the expected  $(Ti + Fe^{3+})$  vs.  $O^3O^{2-}$  relation, as  $2 \times M^1Ti^{4+} + M^{(1,3)}Fe^{3+} \sim 1.0$  apfu.

When considering the possible sequences along the  $a^*$ -direction, again several combinations are possible; however, only a few of these can reproduce the  $OH:O^{2-}$  ratio close to 1:1. In this connection, we recall that the relative intensities of the bands associated with  $OH-OH$  and  $OH-O^{2-}$  configurations (see above) are compatible with a statistical distribution between  $OH$  and  $O^{2-}$  in the structure of the examined samples.

The  $OH$ -spectra show only the absorptions due to  $OH-OH$  and  $OH-O^{2-}$  inter-strip configurations, and thus a significant part of the puzzle, i.e., the  $O^{2-}-O^{2-}$  configurations, are invisible to this technique. Hence, complete information on the short-range order of cations based on the band intensity is not possible. However, inspection of Figure 3 suggests that the  $OH \cdots Na \cdots OH$  configurations are predominantly of the type  $MgMgMg$  or  $MgMgM^{3+}$  with  $M^{3+}$  equal to Al, whereas the  $OH \cdots Na \cdots O^{2-}$  configurations are predominantly of the type  $MgMgAl$  coupled with  $TiMgMg$ ,  $Fe^{3+}Fe^{3+}Mg$  or  $Fe^{3+}MgMg$ . Thus, short-range order of both cations and anions is extensive in these amphiboles.

#### ACKNOWLEDGMENTS

Alberto Zanetti kindly provided the single crystals used in his 1996 paper. F.C.H. was supported by a Canada Research Chair in Crystallography and Mineralogy, by Natural Sciences and Engineering Research Council of Canada

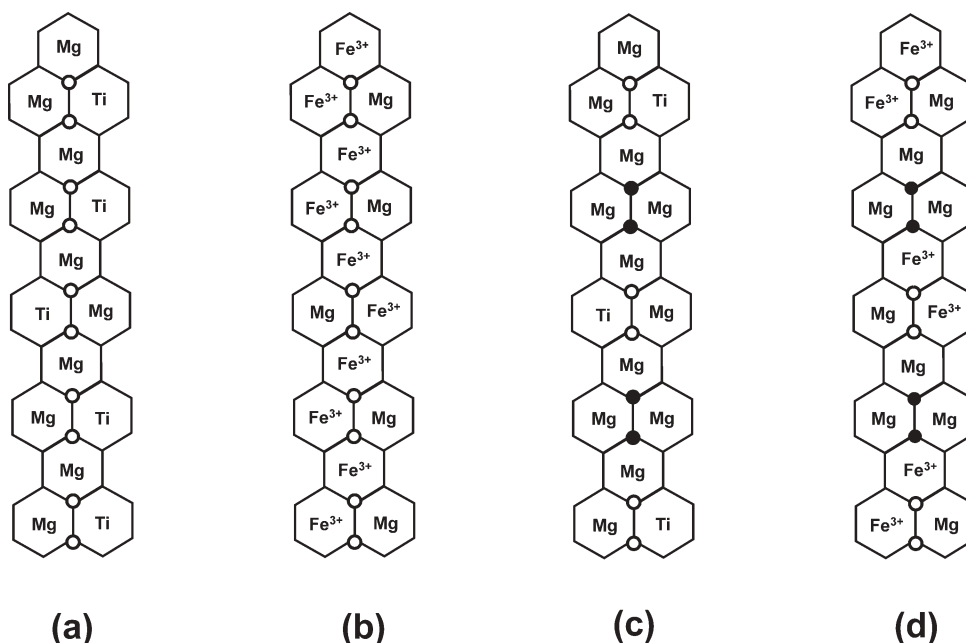


FIGURE 6. Schematic combinations of local arrangements for the M1, M3, and O3 sites within the strip of octahedra in Ti-bearing pargasite; for explanation see text. Full circle = OH, hollow circle =  $O^{2-}$ .

Discovery, Research Tools and Equipment, and Major Facilities Access grants, and by Canada Foundation for Innovation grants. R.O. acknowledges funding from IGG-CNR through the project TA01.04.02. Positive criticism of referees D.M. Jenkins, M. Welch, E. Libowitzky, and M. Gottschalk helped to improve the clarity of the manuscript.

### REFERENCES CITED

- Addison, C.C., Addison, W.E., Neal, G.H., and Sharp, J.H. (1962a) Amphiboles. I. The oxidation of crocidolite. *Journal of Chemical Society*, 1962, 1468–1471.
- Addison, W.E., Neal, G.H., and Sharp, J.H. (1962b) Amphiboles. II. The kinetics of oxidation of crocidolite. *Journal of Chemical Society*, 1962, 1472–1475.
- Barnes, V.E. (1930) Changes in hornblende at about 800 °C. *American Mineralogist*, 15, 393–417.
- Della Ventura, G., Robert, J.-L., Bény, J.-M., Raudsepp, M., and Hawthorne, F.C. (1993) The OH-F substitution in Ti-rich potassium-richterites: Rietveld structure refinement and FTIR and micro-Raman spectroscopic studies of synthetic amphiboles in the system  $K_2O-Na_2O-CaO-MgO-SiO_2-TiO_2-H_2O-HF$ . *American Mineralogist*, 78, 980–987.
- Della Ventura, G., Robert, J.-L., and Hawthorne, F.C. (1996) Infrared spectroscopy of synthetic (Ni,Mg,Co)-potassium-richterite. In M.D. Dyar, C. McCammon, and M.W. Schaefer, Eds., *Mineral Spectroscopy: a Tribute to Roger G. Burns*, p. 55–63. The Geochemical Society Special Publication No. 5, Houston, Texas.
- Della Ventura, G., Hawthorne, F.C., Robert, J.-L., Delbove, F., Welch, M.D., and Raudsepp, M. (1999) Short-range order of cations in synthetic amphiboles along the richterite–pargasite join. *European Journal of Mineralogy*, 11, 79–94.
- Della Ventura, G., Robert, J.-L., Sergent, J., Hawthorne, F.C., and Delbove, F. (2001) Constraints on F vs. OH incorporation in synthetic  $^{69}Al$ -bearing monoclinic amphiboles. *European Journal of Mineralogy*, 13, 841–847.
- Ernst, W.G. and Wai, C.M. (1970) Mössbauer, infrared, X-ray, and optical study of cation ordering and dehydroxylation in natural and heat-treated sodic amphiboles. *American Mineralogist*, 55, 1226–1258.
- Gottschalk, M., Andrut, M., and Melzer, S. (1999) The determination of the cumingtonite content of synthetic tremolite. *European Journal of Mineralogy*, 11, 967–982.
- Hawthorne, F.C. (1997) Short-range order in amphiboles: a bond-valence approach. *Canadian Mineralogist*, 35, 201–216.
- Hawthorne, F.C., Oberti, R., Cannillo, E., Sardone, N., Zanetti, A., Grice, J.D., and Ashley, P.M. (1995) A new anhydrous amphibole from the Hoskins mine, Grenfell, New South Wales, Australia: description and crystal structure of ungaretitite,  $NaNa_2(Mn_3^{2+}Mn_3^{3+})Si_8O_{22}O_2$ . *American Mineralogist*, 80, 165–172.
- Hawthorne, F.C., Della Ventura, G., Robert, J.-L., Welch, M.D., Raudsepp, M., and Jenkins, D.M. (1997) A Rietveld and infrared study of synthetic amphiboles along the potassium-richterite-tremolite join. *American Mineralogist*, 82, 708–716.
- Hawthorne, F.C., Oberti, R., Zanetti, A., and Czamanske, G.K. (1998) The role of Ti in hydrogen-deficient amphiboles: sodic-calcic and sodic amphiboles from Coyote Peak, California. *Canadian Mineralogist*, 36, 1253–1265.
- Hawthorne, F.C., Cooper, M.A., Grice, J.D., and Ottolini, L. (2000a) A new anhydrous amphibole from the Eifel region, Germany: description and crystal structure of obertiite,  $NaNa_2(Mg_2Fe^{3+}Ti^{4+})Si_8O_{22}O_2$ . *American Mineralogist*, 85, 236–241.
- Hawthorne, F.C., Welch, M.D., Della Ventura, G., Liu, S., Robert, J.-L., and Jenkins, D.M. (2000b) Short-range order in synthetic aluminous tremolites: An infrared and triple-quantum MAS NMR study. *American Mineralogist*, 85, 1716–1724.
- Hawthorne, F.C., Della Ventura, G., Oberti, R., Robert, J.-L., and Iezzi, G. (2005) Short-range order in minerals: Amphiboles. *Canadian Mineralogist*, 43, 1895–1920.
- Jirak, Z., Pechar, F., and Vratislav, S. (1986) Distribution of cations and the proton location in kaersutite. *Crystallographic Research and Technology*, 21, 1517–1519.
- Kitamura, M. and Tokonami, M. (1971) The crystal structure of kaersutite. *Science Reports Tohoku University Series 3*, 11, 125–141.
- Kitamura, M., Tokonami, M., Koto, K., Horiuchi, H., and Morimoto, N. (1973) Cation ordering in kaersutite by neutron diffraction. *Journal of the Mineralogical Society of Japan*, 11, 49.
- Kitamura, M., Tokonami, M., and Morimoto, N. (1975) Distribution of titanium atoms in oxy-kaersutite. *Contribution to Mineralogy and Petrology*, 51, 167–172.
- Leake, B.E. (1968) A catalog of analysed calciferous and subcalciferous amphiboles together with their nomenclature and associated minerals. *Geological Society of America Special Papers*, 98, 210 p. Boulder, Colorado.
- Oberti, R., Ungaretti, L., Cannillo, E., and Hawthorne, F.C. (1992) The behaviour of Ti in amphiboles. I. Four- and six-coordinate Ti in richterite. *European Journal of Mineralogy*, 3, 425–439.
- Oberti, R., Hawthorne, F.C., Ungaretti, L., and Cannillo, E. (1995)  $^{69}Al$  disorder in amphiboles from mantle peridotite. *Canadian Mineralogist*, 33, 867–878.
- Pechar, F., Fuess, H., and Joswig, W. (1989) Refinement of the crystal structure of kaersutite (Vičí Hora, Bohemia) from neutron diffraction. *Neues Jahrbuch Mineral Monatshefte*, 134–143.
- Phillips, M.W., Draheim, J.E., Popp, R.K., Clowe, C.A., and Pinkerton, A.A. (1989) Effects of oxidation-dehydrogenation in tschermakitic hornblende. *American Mineralogist*, 74, 764–773.
- Popp, R.K., Virgo, D., Yoder, H.D., Hoernig, J.T.C., and Phillips, M.W. (1995a) An experimental study of phase equilibria and Fe oxy-component in kaersutitic amphibole: Implications for the  $f_{H_2}$  and  $a_{H_2O}$  in the upper mantle. *American Mineralogist*, 80, 534–548.
- Popp, R.K., Virgo, D., and Phillips, M. (1995b) H deficiency in kaersutitic amphiboles: experimental verification. *American Mineralogist*, 80, 1347–1350.
- Raudsepp, M., Turnok, A.C., Hawthorne, F.C., Sheriff, B.L., and Hartman, J.S. (1987) Characterization of synthetic pargasitic amphiboles ( $NaCa_2Mg_3M^{3+}Si_6Al_2O_{22}(OH,F)_2$ ;  $M^{3+} = Al, Cr^{3+}, Ga, Fe^{3+}, Sc, In$ ) by infrared spectroscopy, Rietveld structure refinement, and  $^{27}Al$  and  $^{29}Si$  MAS NMR spectroscopy. *American Mineralogist*, 72, 580–593.
- Robert, J.-L., Della Ventura, G., and Hawthorne, F.C. (1999) Near-infrared study of short-range disorder of OH and F in monoclinic amphiboles. *American Mineralogist*, 84, 86–91.
- Robert, J.-L., Della Ventura, G., Welch, M., and Hawthorne, F.C. (2000) The OH-F substitution in synthetic pargasite at 1.5 kbar, 850 °C. *American Mineralogist*, 85, 926–931.
- Saxena, S.K. and Ekstrom, T.K. (1970) Statistical chemistry of calcic amphiboles. *Contribution to Mineralogy and Petrology*, 26, 276–284.
- Semet, M.P. (1973) A crystal chemical study of synthetic magnesiohastingsite. *American Mineralogist*, 58, 480–494.
- Skogby, H. and Rossman, G.R. (1991) The intensity of amphibole OH bands in the infrared absorption spectrum. *Physics and Chemistry of Minerals*, 18, 64–68.
- Strens, R.S.J. (1974) The common chain, ribbon and ring silicates. In V.C. Farmer, Ed., *The Infrared Spectra of Minerals*, 4, p. 305–330. Mineralogical Society Monograph, London.
- Tait, K.T., Hawthorne, F.C., and Della Ventura, G. (2001) Al-Mg disorder in a gem-quality pargasite from Baffin Island, Nanavut, Canada. *Canadian Mineralogist*, 39, 1725–1732.
- Tait, K.T., Hawthorne, F.C., Grice, J.D., Ottolini, L., and Nayak, V.K. (2005) Dellaventuraitite,  $NaNa_2(MgMn_3^{2+}Ti^{4+}Li)Si_8O_{22}O_2$ , a new anhydrous amphibole from the Kajlidongri manganese mine, Jhabua District, Madhya Pradesh, India. *American Mineralogist*, 90, 304–309.
- Tiepolo, M., Zanetti, A., and Oberti, R. (1999) Detection, crystal-chemical mechanisms and petrological implications of  $^{69}Ti^{4+}$  partitioning in pargasite and kaersutite. *European Journal of Mineralogy*, 11, 345–354.
- Ungaretti, L. (1980) Recent developments in X-ray single crystal diffractometry applied to the crystal-chemical study of amphiboles. *Godišnjak Jugoslavenskog za kristalografiju*, 15, 29–65.
- Zanetti, A., Vannucci, R., Bottazzi, P., Oberti, R., and Ottolini, L. (1996) Infiltration metasomatism at Lherz as monitored by systematic ion-microprobe investigations close to a hornblendite vein. *Chemical Geology*, 134, 113–133.

MANUSCRIPT RECEIVED DECEMBER 22, 2005

MANUSCRIPT ACCEPTED MAY 9, 2007

MANUSCRIPT HANDLED BY EUGEN LIBOWITZKY